

# Shock Acceleration Model with Postshock Turbulence for Radio Relics

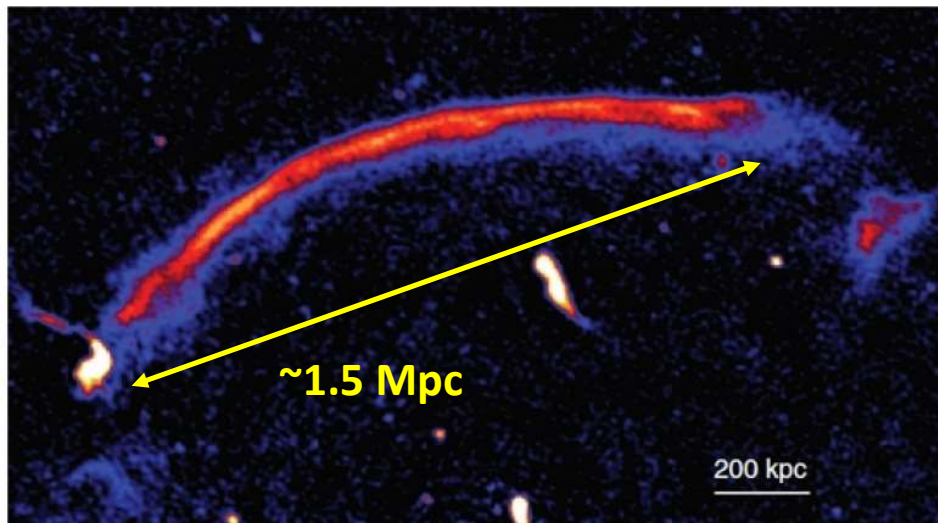
Hyesung Kang (Pusan National Univ., Korea)

Dongsu Ryu (UNIST, Korea)

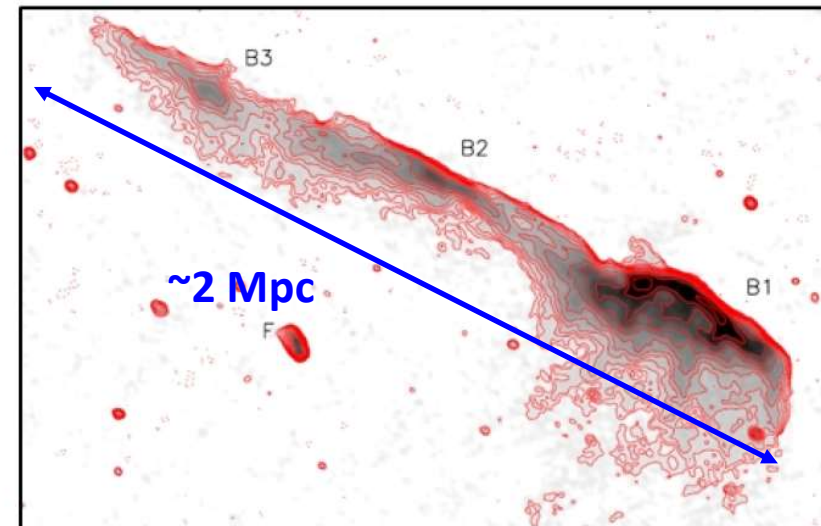
T. W. Jones (Univ. of Minnesota, USA)

Kang, Ryu, Jones,  
2017, ApJ

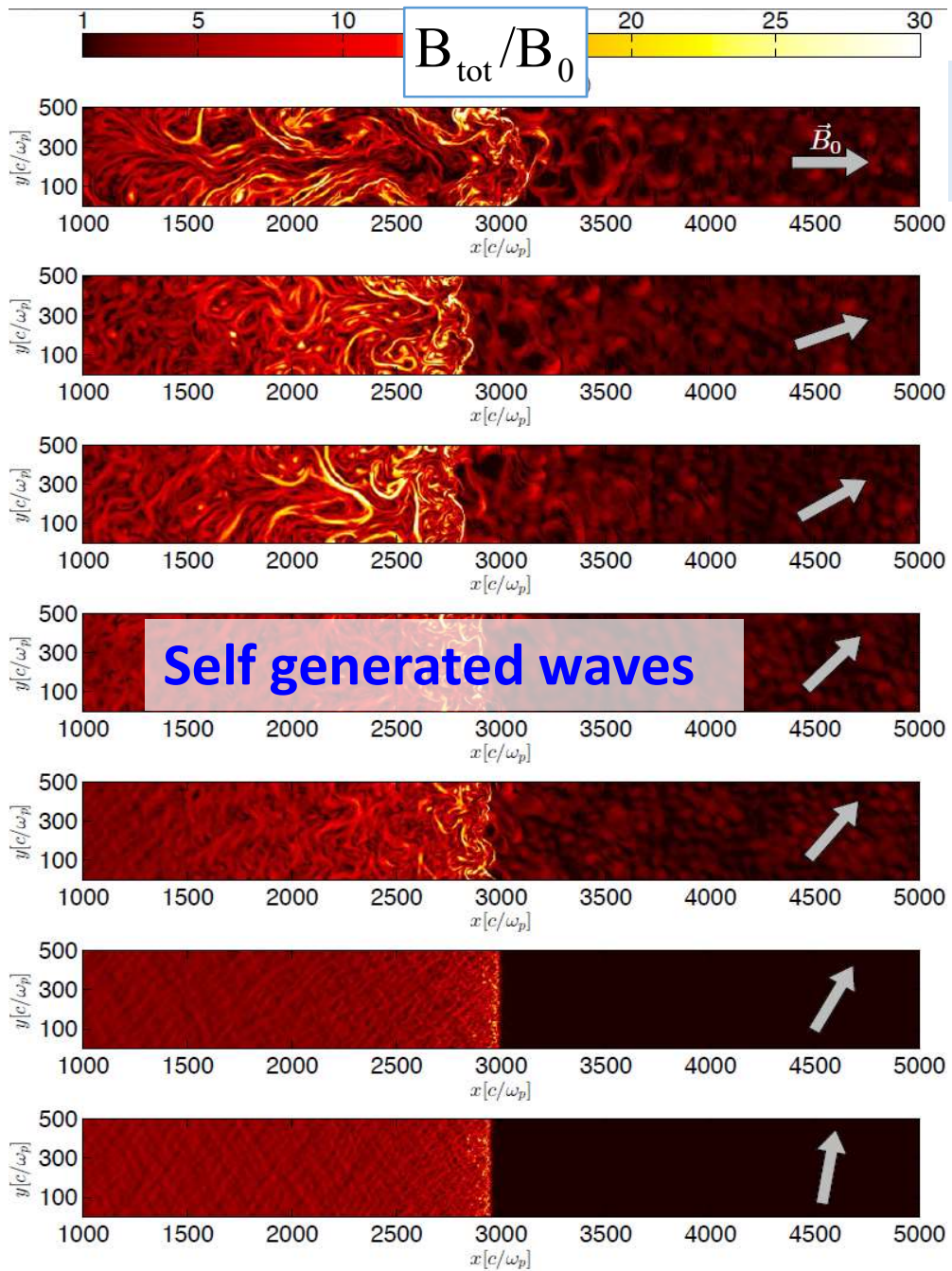
Sausage Relic in CIZA J2242.8+5301



Toothbrush Relic in 1RXS J0603.3+4214



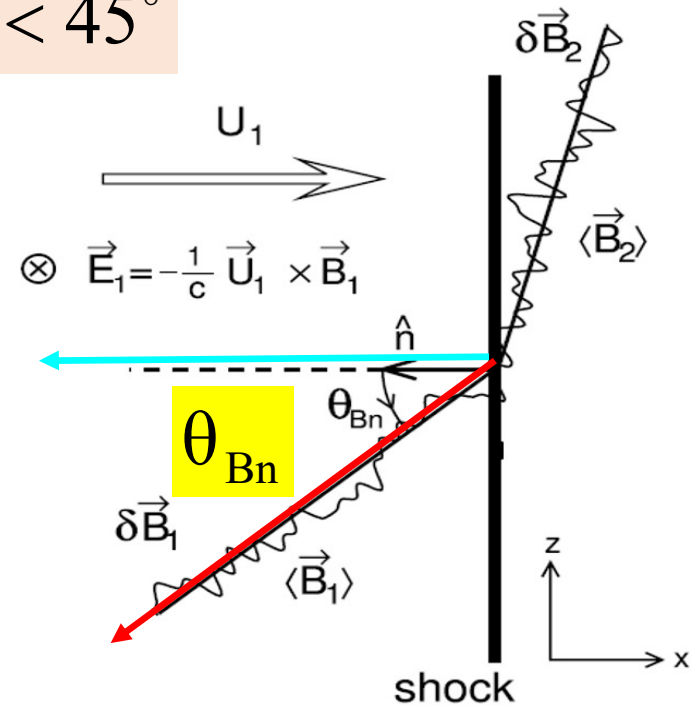
Diffuse radio sources on Mpc scales detected in the outskirts of galaxy clusters: synchrotron radiation emitted by  $\sim$ GeV electrons accelerated at **structure formation shocks via DSA (Fermi I) process.**



Characteristics of collisionless shocks depend on B field direction

Quasi-parallel= Q-par

$$\theta_{Bn} < 45^\circ$$



Quasi-perpendicular= Q-perp

$$\theta_{Bn} > 45^\circ$$

Hybrid simulations by Caprioli & Spitkovsky 2014

## Properties of Astrophysical Plasmas

	solar wind (IPM)	ISM	ICM	solar flare
$n_H$ (cm <sup>-3</sup> )	5	0.1	10 <sup>-4</sup>	10 <sup>10</sup>
$T$ (°K)	10 <sup>5</sup>	10 <sup>4</sup>	5x10 <sup>7</sup>	10 <sup>5</sup> -10 <sup>6</sup>
$B$ (μG)	50	5	1	10 <sup>8</sup>
$c_s$ (km/s)	50	15	1000	50-150
$v_A$ (km/s)	40	30	180	2000
$\beta_p = P_g/P_B$	1.6	0.3	40	0.01
$\alpha_p = \omega_{pe}/\Omega_e$	140	200	30	3
$u_s$ (km/s)	500	3000	2000	-
$M_s = u_s/c_s$	10	200	2	-
$M_A = u_s/v_A$	13	100	11	-

**IPM**

=InterPlanetary Medium

**ISM**

=InterStellar Medium

**ICM**

=IntraCluster Medium

$$\beta_p = \frac{P_{gas}}{P_B} \propto \frac{n_H T}{B^2}$$

$$\alpha_p = \frac{\omega_{p,e}}{\Omega_{c,e}} \propto \frac{\sqrt{n_e}}{B}$$

$$M_A \approx \beta_p^{1/2} M_s$$

$\theta_{Bn}$  : obliquity angle

ICM (cluster shocks) vs ISM (SNR shocks)

higher  $\beta_p$  : B pressure is dynamically less important in ICM

lower  $\alpha_p$  : wave - part. interactions and stochastic acceleration more significant in ICM

particle acceleration at collisionless shocks depend on  $M_s, M_A, \theta_{Bn}, \beta_p, \alpha_p$

## Particle Acceleration Processes at collisionless shocks

### (1) Diffusive Shock Acceleration (DSA): Fermi 1<sup>st</sup> order process

- effective at **quasi-parallel (Q-par)** shocks
- scattering off MHD waves in the upstream and downstream region

### (2) Shock Drift Acceleration (SDA)

- effective at **quasi-perpendicular (Q-perp)** shocks
- drifting along the convective E field (grad B) at the shock front

$$\vec{E}_{conv} = -\frac{1}{c} \vec{V} \times \vec{B}_0$$

### (3) Shock Surface Acceleration (SSA)

- effective at **quasi-perpendicular (Q-perp)** shocks
- reflected by shock potential, scattered by upstream waves
- moving along the convective E field, while being trapped at the shock foot

### (4) Turbulent Acceleration (TA): Fermi 2<sup>nd</sup> order, stochastic acceleration

- much less efficient than Fermi I
- could be important in turbulent plasmas

### (5) Turbulent Reconnection (TR) of Magnetic Fields

**Essential ingredients:**  $\vec{B}_0$  &  $\delta\vec{B}$

## DSA: Fermi first order process

MHD waves in a converging flow act as converging mirrors

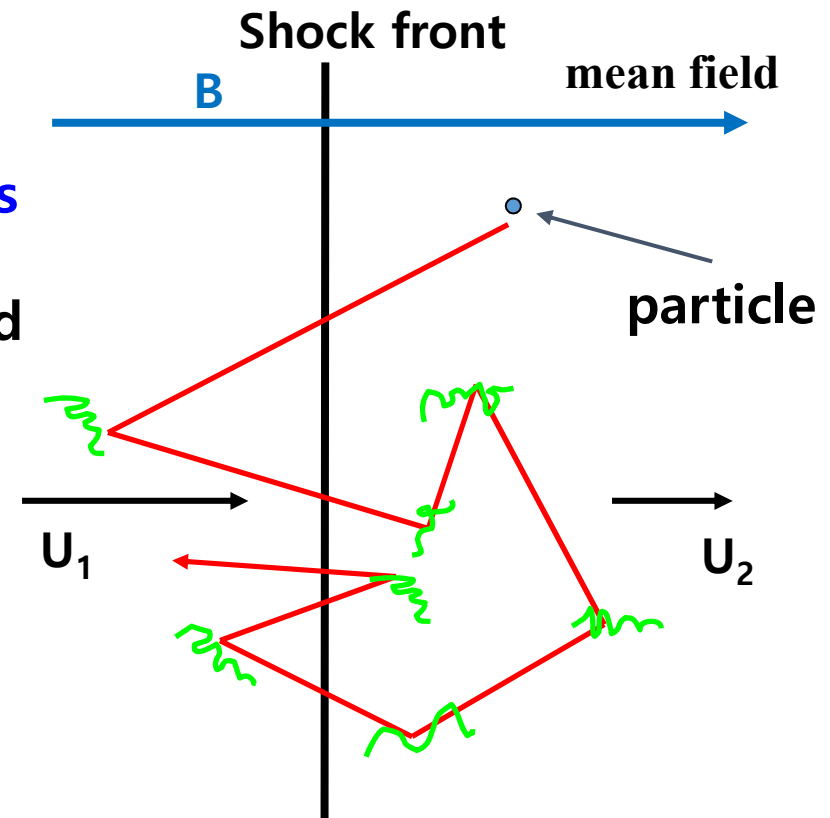
- particles are scattered & isotropized by waves in local fluid frame
- cross the shock many times

$$\frac{\Delta p}{p} \sim \frac{u_1 - u_2}{v} \text{ at each shock crossing}$$

test - particle limit solution

$$f_{\text{test}}(p) \propto p^{-q_{\text{test}}} : \text{power - law}$$

$$q_{\text{test}} = \frac{3u_1}{(u_1 - u_2)} = \frac{4M_s^2}{M_s^2 - 1}$$



radio synchrotron emission

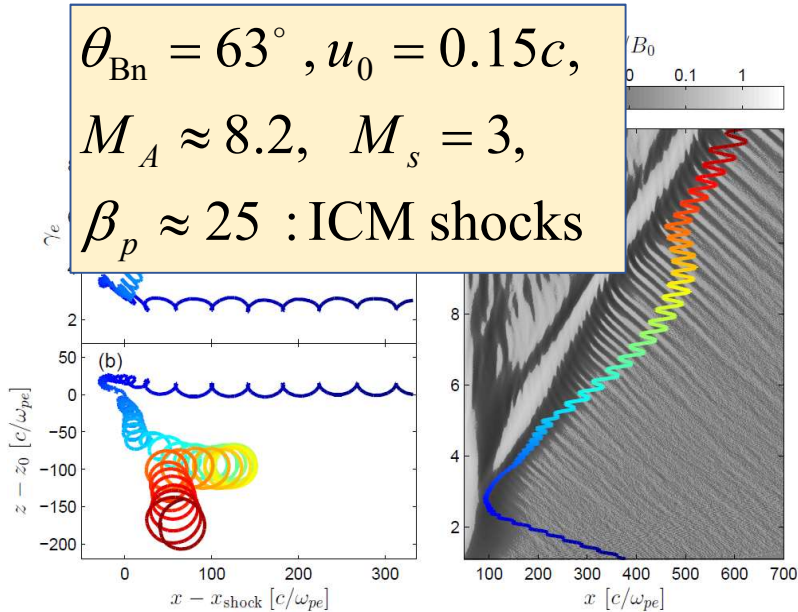
$$j_\nu \propto \nu^{-\alpha}$$

$$\alpha = \frac{q - 3}{2} = \frac{M_s^2 + 3}{2(M_s^2 - 1)}$$

# PIC simulations of Q-perp shocks (high $\beta$ )

Guo, Sironi, & Narayan 2014

$\theta_{Bn} = 63^\circ$ ,  $u_0 = 0.15c$ ,  
 $M_A \approx 8.2$ ,  $M_s = 3$ ,  
 $\beta_p \approx 25$  : ICM shocks



## Evolution of an electron undergoing multiple SDA

Reflection of some electrons

due to Magnetic mirror at shock

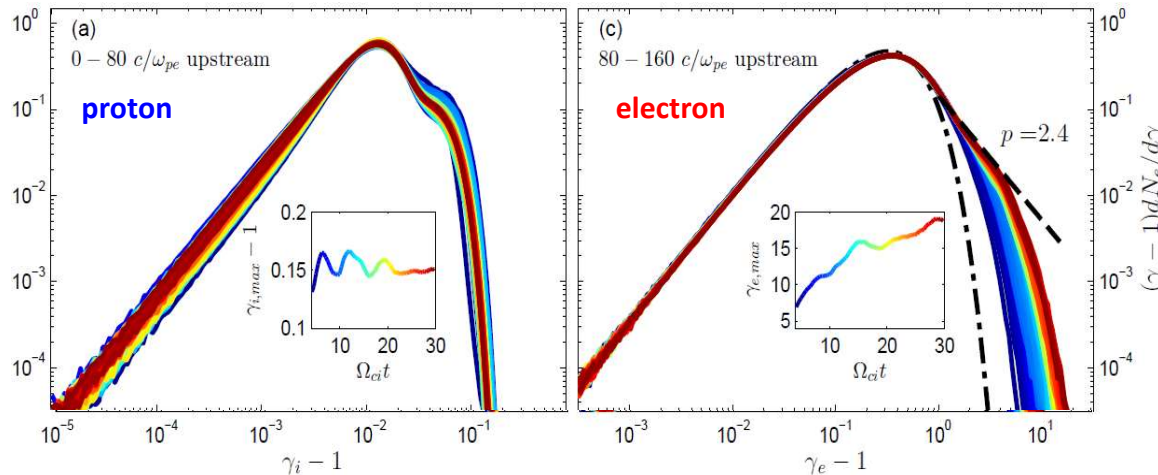
$$T_{\parallel,e} > T_{\perp,e}$$

→ Induce temperature anisotropy in the upstream

→ firehose instability excites waves

→ Reflected electrons are scattered back to the shock downstream by the waves

→ Undergo multiple SDA cycles



## Multiple SDA for electrons

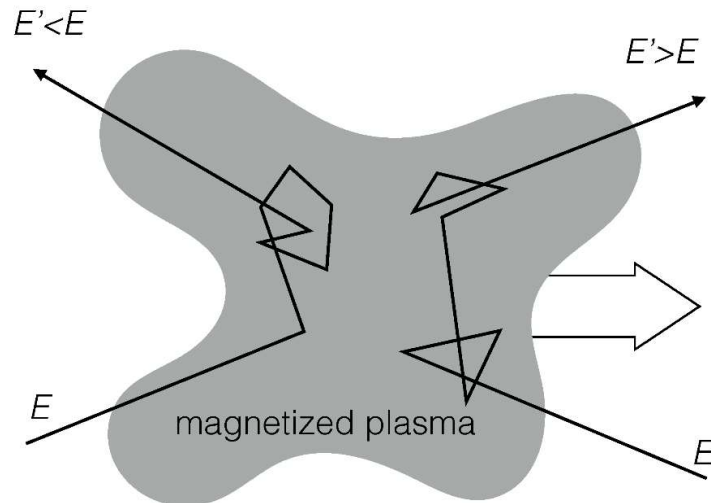
→ suprathermal tail

→ Pre-acceleration for DSA

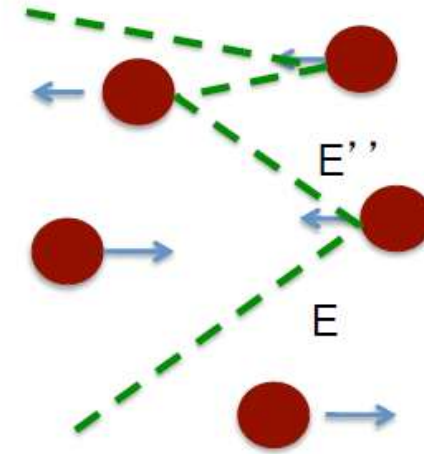
→ injected to Fermi I

Energy spectrum

## Fermi 2nd order process= Turbulent acceleration



$$\frac{\Delta E}{E} \sim \left(\frac{V}{c}\right)^2$$



Scatterings by turbulence  
(randomly moving clouds)

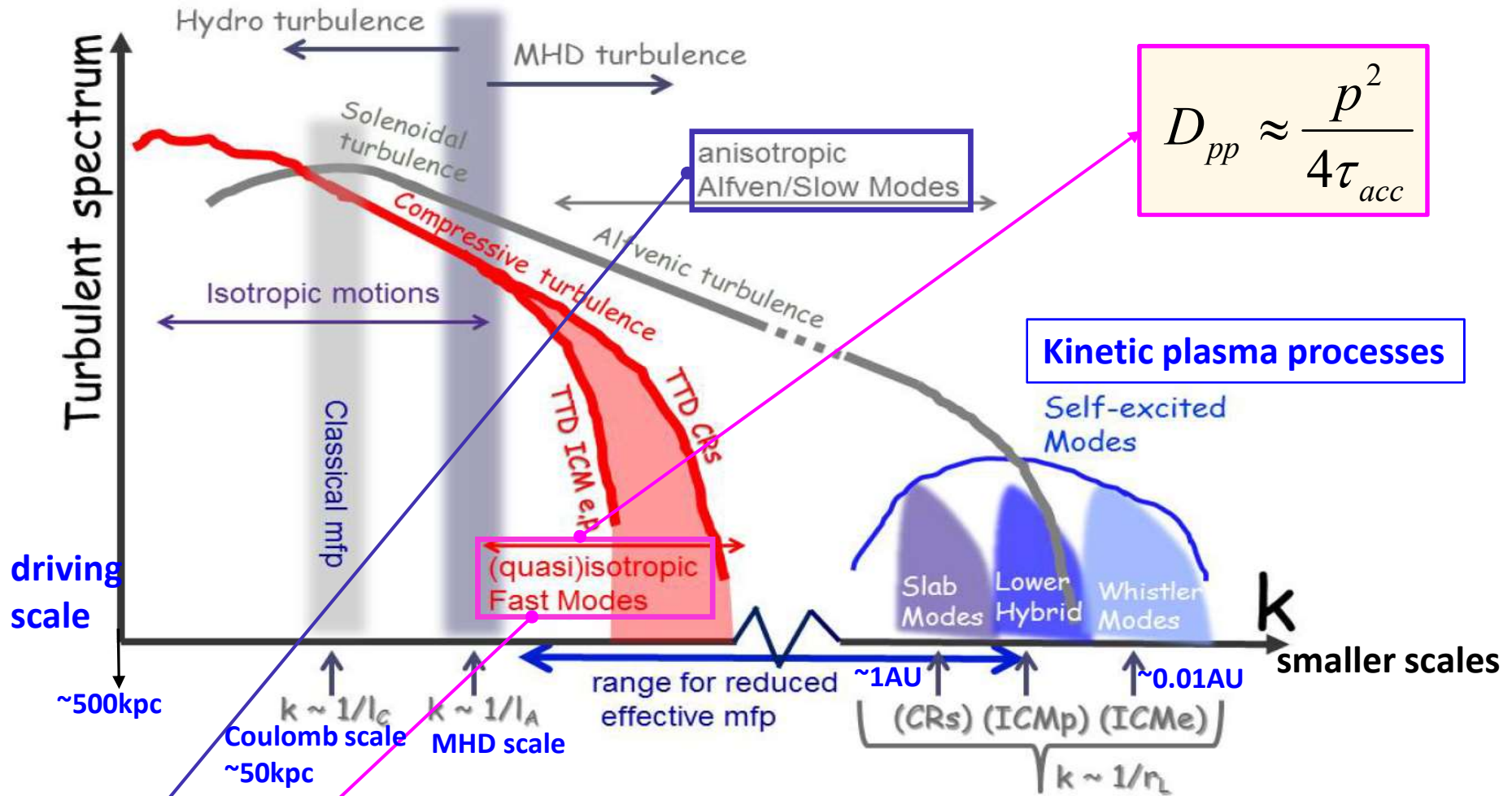
Fermi 1949

Stochastic energy gain in collisions with MHD/plasma waves  
(**head-on** collisions are more frequent than **over-taking** collisions)  
→ 2<sup>nd</sup> order in energy gain (slow and inefficient)

CR particles (protons + electrons) could be accelerated via **Fermi II** acceleration **by turbulence in ICM**.

# Power-spectrum of Turbulence in the ICM

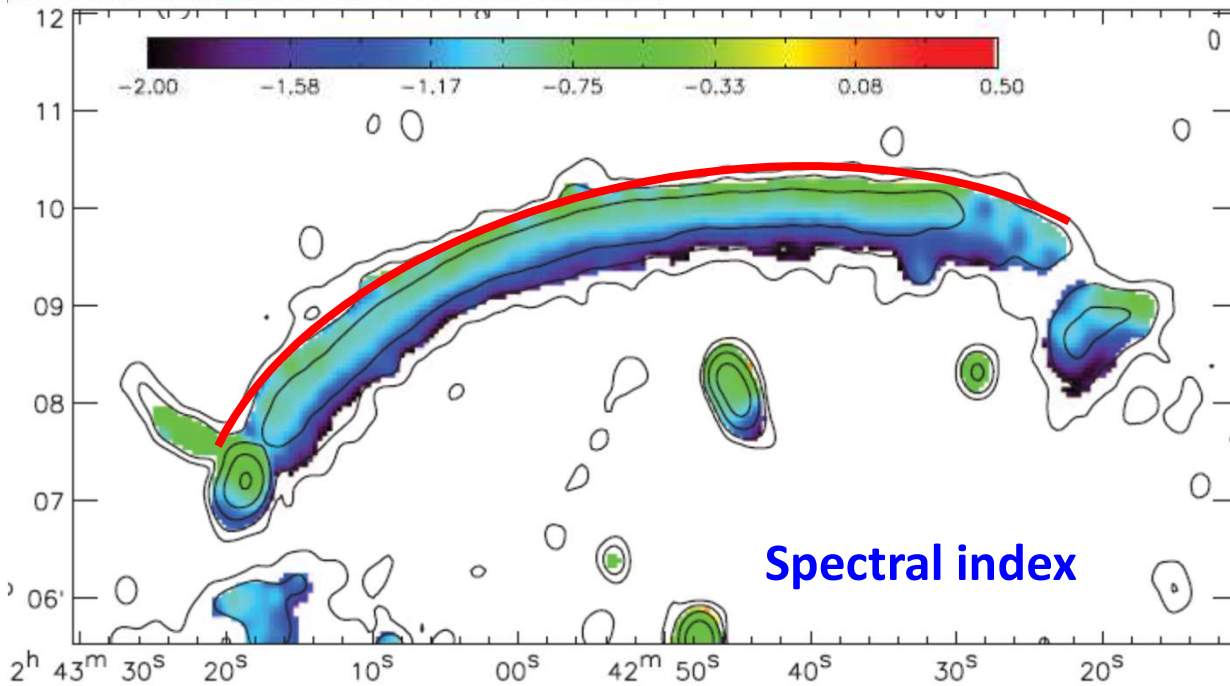
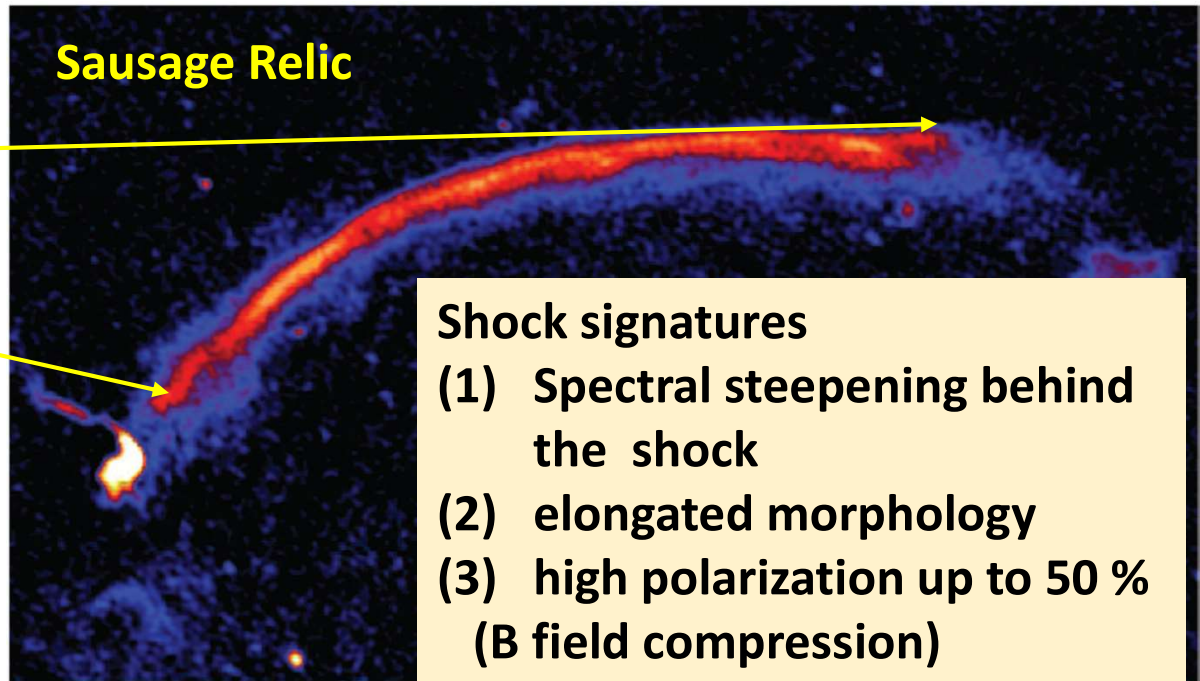
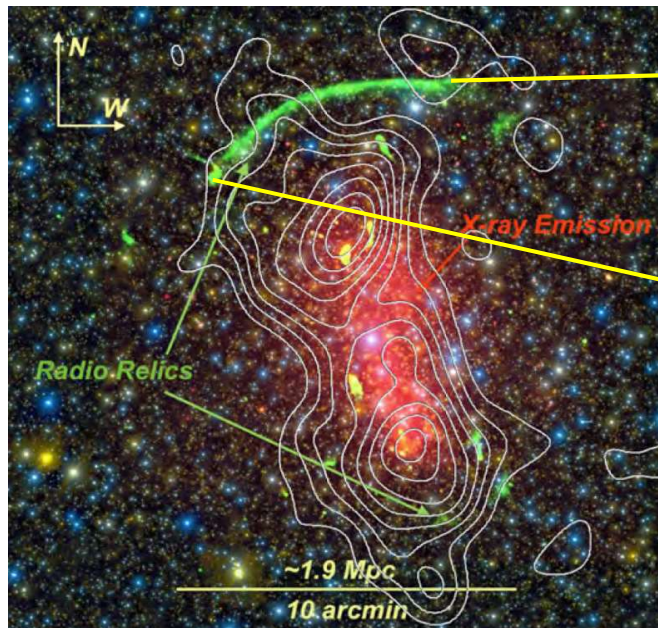
Brunetti & Lazarian 2011  
Brunetti & Jones 2014



- Alfvén and slow modes become anisotropic at small scales, so scattering by Alfvénic turbulence becomes inefficient. (Cho & Lazarian 2003)
- But **fast mode** remains isotropic at small scales, so **Transit Time Damping (TTD)** with fast modes is dominant in ICM (Brunetti & Lazarian 2007)



# cluster CIZAJ2242.8+5301



$$F_\nu \propto \nu^{-\alpha}$$

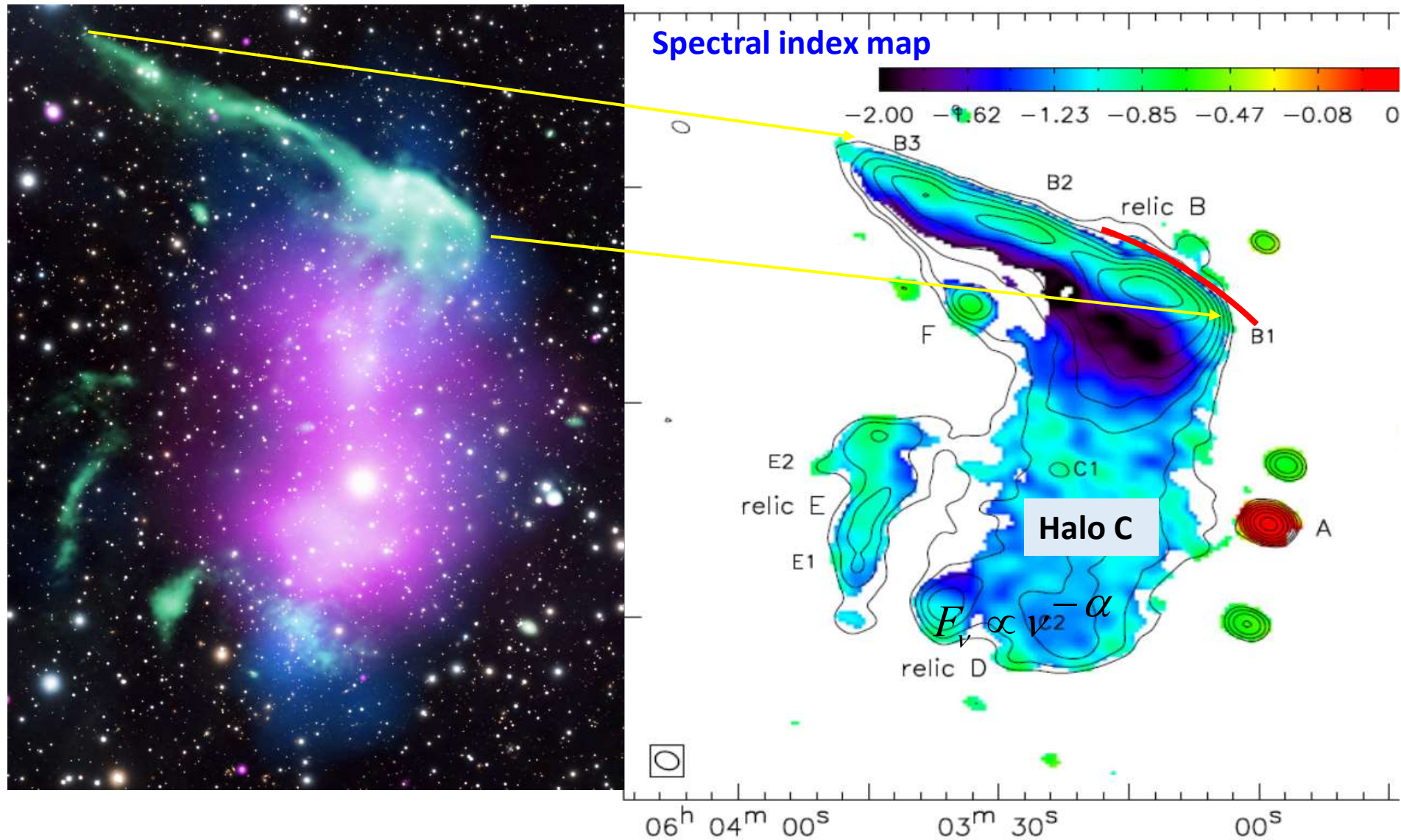
$$M_{radio}^2 = \frac{(3 + 2\alpha_{sh})}{(2\alpha_{sh} - 1)}$$

$$M_{radio} \approx 4.6$$

but  $M_X \approx 2.7$  from

$$\frac{T_2}{T_1} = \frac{(M_X^2 + 3)(5M_X^2 - 1)}{16M_X^2}$$

cluster 1RXS J060303.3 **Toothbrush Relic**



$$M_{radio}^2 = \frac{(3 + 2\alpha_{sh})}{(2\alpha_{sh} - 1)} \Rightarrow M_{radio} \approx 2.8 \quad \text{but} \quad M_X \approx 1.5$$

# Reacceleration Model for Formation of Giant Radio Relics

CR electrons in lobes of AGN jet

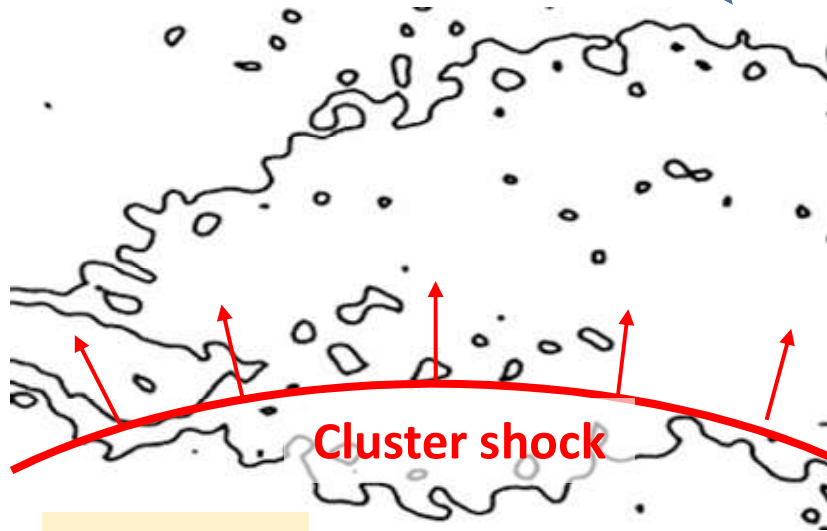
~ Gyr ago



Cooled Fossil electrons with  $\gamma_e < 300$

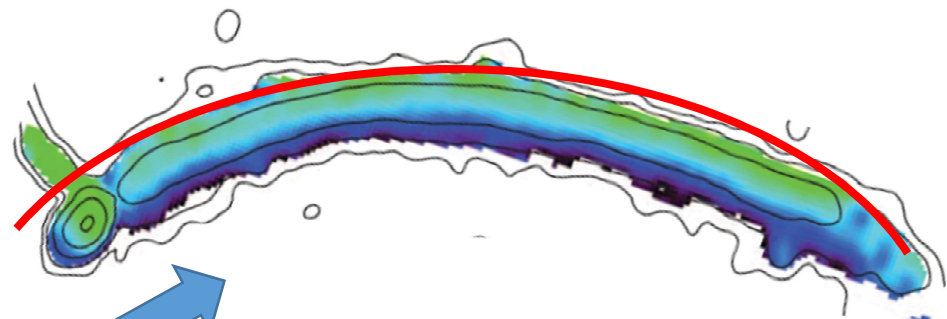
$$f_{\text{pre}}(p) = f_o \cdot p^{-s} \exp \left[ - \left( \frac{p}{p_{e,c}} \right)^2 \right]$$

provide seed CR electrons to DSA



Cluster shock

$$M_s \approx 3.0$$



## DSA simulations in test-particle limit

in a **co-expanding** frame which expands with **1D spherical shock**.

$$\frac{\partial \tilde{\rho}}{\partial t} + \frac{1}{a} \frac{\partial (v \tilde{\rho})}{\partial x} = -\frac{2}{ax} \tilde{\rho} v \quad \text{ordinary gasdynamic Eqs (high beta)}$$

$$\frac{\partial (\tilde{\rho} v)}{\partial t} + \frac{1}{a} \frac{\partial (\tilde{\rho} v^2 + \tilde{P}_g)}{\partial x} = -\frac{2}{ax} \tilde{\rho} v^2 - \frac{\dot{a}}{a} \tilde{\rho} v - \ddot{a} x \tilde{\rho}$$

$$\frac{\partial (\tilde{\rho} \tilde{e}_g)}{\partial t} + \frac{1}{a} \frac{\partial (\tilde{\rho} \tilde{e}_g v + \tilde{P}_g v)}{\partial x} = -\frac{2}{ax} (\tilde{\rho} \tilde{e}_g v + \tilde{P}_g v) - 2 \frac{\dot{a}}{a} \tilde{\rho} \tilde{e}_g - \ddot{a} x \tilde{\rho} v - \tilde{L}(x, t)$$

$x = r/a$  : co-moving coordinate,  $a$  = expansion factor

## CR transport Equation for electron distribution function

$$\frac{\partial g_e}{\partial t} + u \frac{\partial g_e}{\partial r} = \frac{1}{3r^2} \frac{\partial (r^2 u)}{\partial r} \left( \frac{\partial g_e}{\partial y} - 4g_e \right) \quad g_e = f_e \cdot p^4, \quad y = \ln(p / m_e c)$$

$$+ \frac{1}{r^2} \frac{\partial}{\partial r} \left[ r^2 \kappa(r, p) \frac{\partial g_e}{\partial r} \right] + p \frac{\partial}{\partial y} \left[ \frac{D_{pp}}{p^3} \left( \frac{\partial g_e}{\partial y} - 4g_e \right) \right] + p \frac{\partial}{\partial y} \left( \frac{b}{p^2} g_e \right)$$

Spatial diffusion  
= Fermi I

Momentum diffusion  
= Fermi II

Coulomb/  
Synchrotron/iC losses

**Table 1.** Parameters for Model Spherical Shocks

Model	$M_X$	$M_{\text{radio}}$	$M_{s,i}$	$kT_1$ (keV)	$B_1$ ( $\mu G$ )	$t_{\text{obs}}$ (Myr)	$M_{s,\text{obs}}$	$kT_{2,\text{obs}}$ (keV)	$u_{s,\text{obs}}$ (km s $^{-1}$ )	$N$ ( $10^{-4}$ )
Sausage	2.7	4.6	4.0	2.1	1	211	3.21	8.6	$2.4 \times 10^3$	1.2
Toothbrush	1.5	2.8	3.6	3.0	1	144	3.03	11.2	$2.7 \times 10^3$	5.0

$M_X$ : Mach number inferred from X-ray observations

$M_{\text{radio}}$ : Mach number estimated from observed radio spectral index at the relic edge

$M_{s,i}$ : initial shock Mach number at the onset of the simulations ( $t_{\text{age}} = 0$ )

$kT_1$ : gas temperature in the preshock ICM

$B_1$ : magnetic field strength in the preshock ICM

$t_{\text{obs}}$ : shock age when the simulated results match the observations

$M_{s,\text{obs}}$ : shock Mach number at  $t_{\text{obs}}$

$kT_{2,\text{obs}}$ : postshock temperature at  $t_{\text{obs}}$

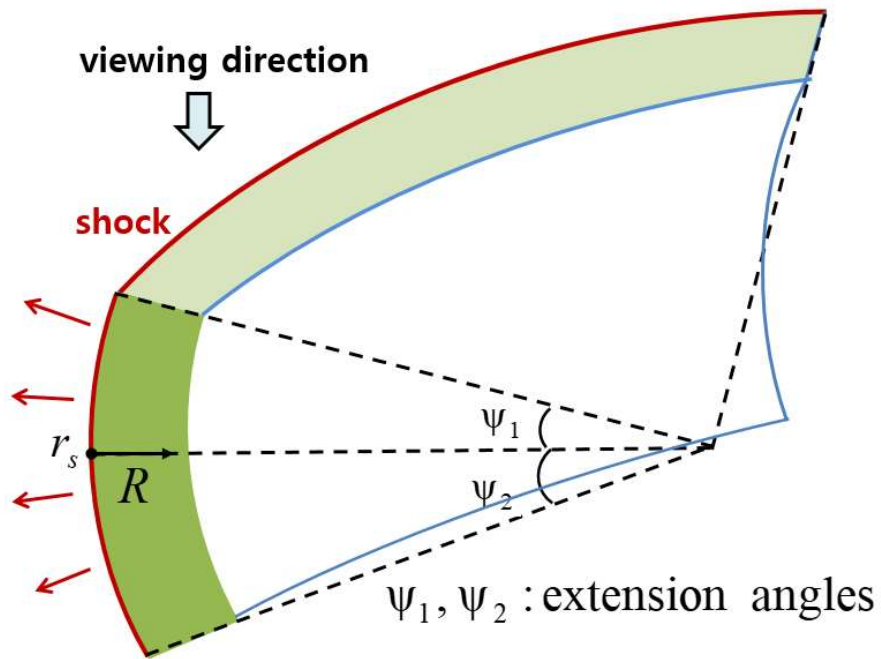
$u_{s,\text{obs}}$ : shock speed at  $t_{\text{obs}}$

$N = P_{\text{CRe}}/P_g$ : the ratio of seed CR electron pressure to gas pressure in the preshock region

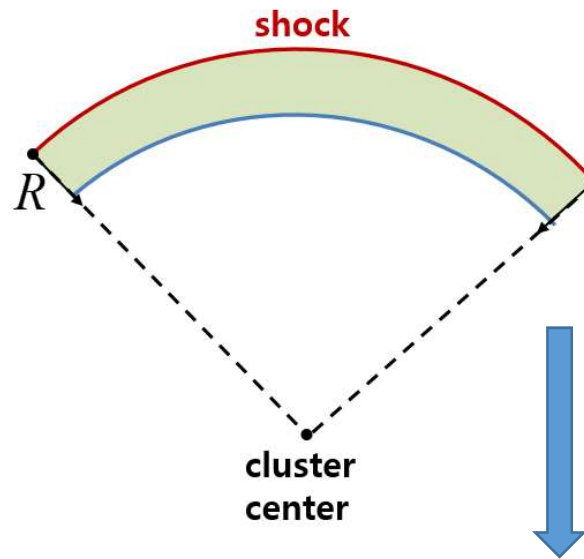
$$D_{pp} \approx \frac{p^2}{4\tau_{\text{acc}}}, \quad \tau_{\text{acc}} \approx 10^8 \text{ yr}$$

**The spherical shock slows down and its Mach number decreases in time.**

(a) 3D structure of the shock surface



(b) 2D Projected image in the sky



## Surface brightness profile

$$I_\nu(R) = \int_0^{h_{1,\max}} j_\nu(r) dh_1 + \int_0^{h_{2,\max}} j_\nu(r) dh_2$$

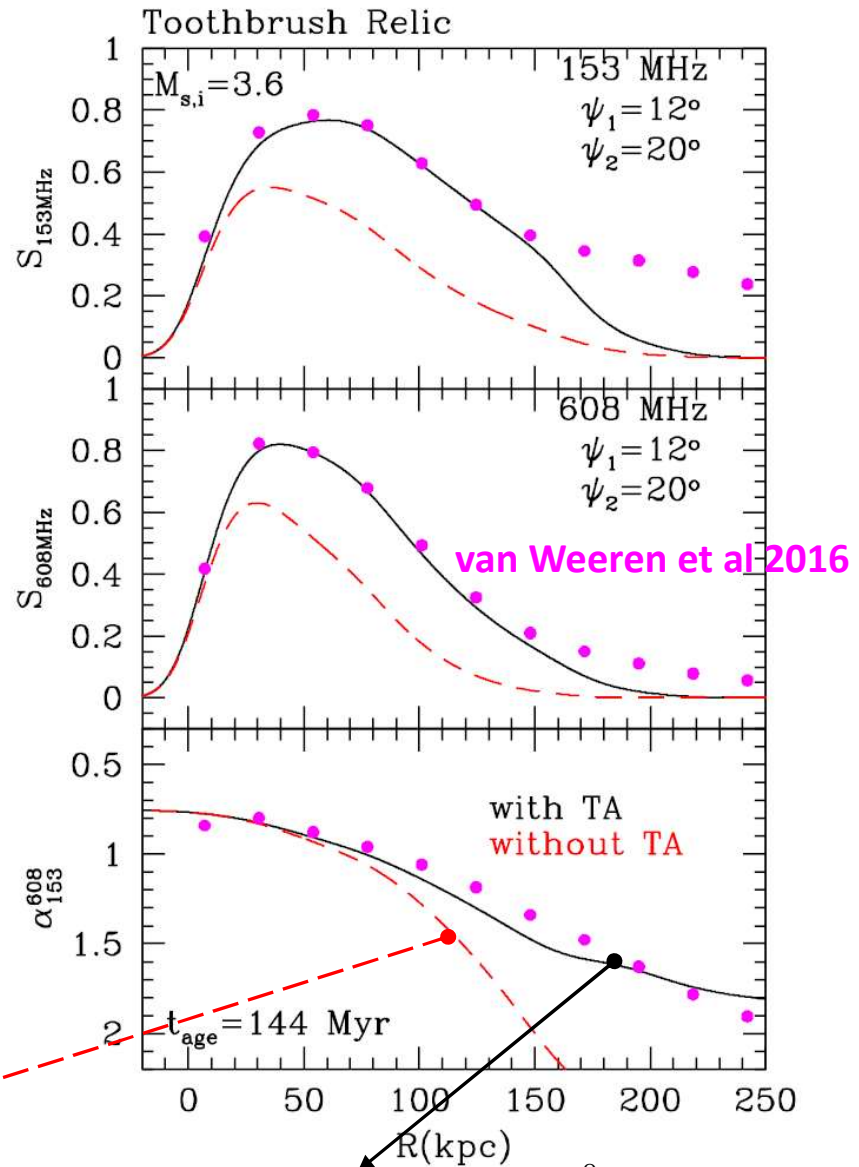
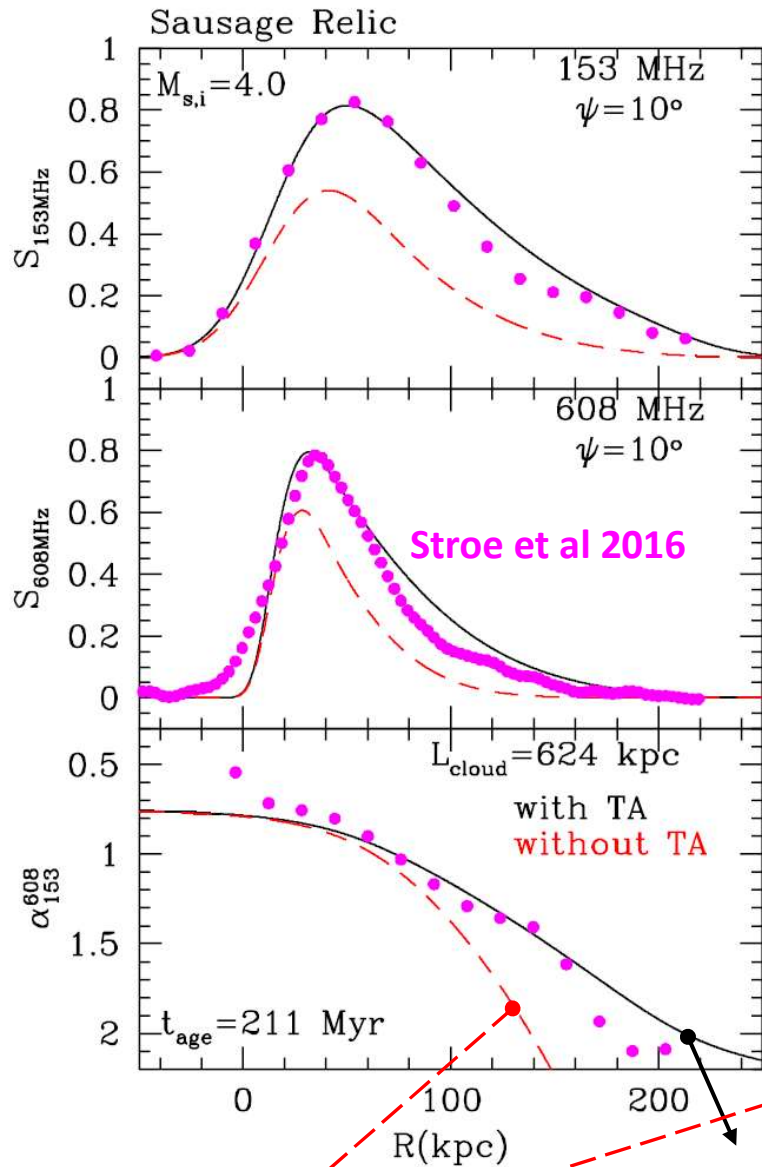
## Radio flux density profile

$$S_\nu(R) = \int_{beam} I_\nu(R) d\Omega$$

Smoothed over telescope beam

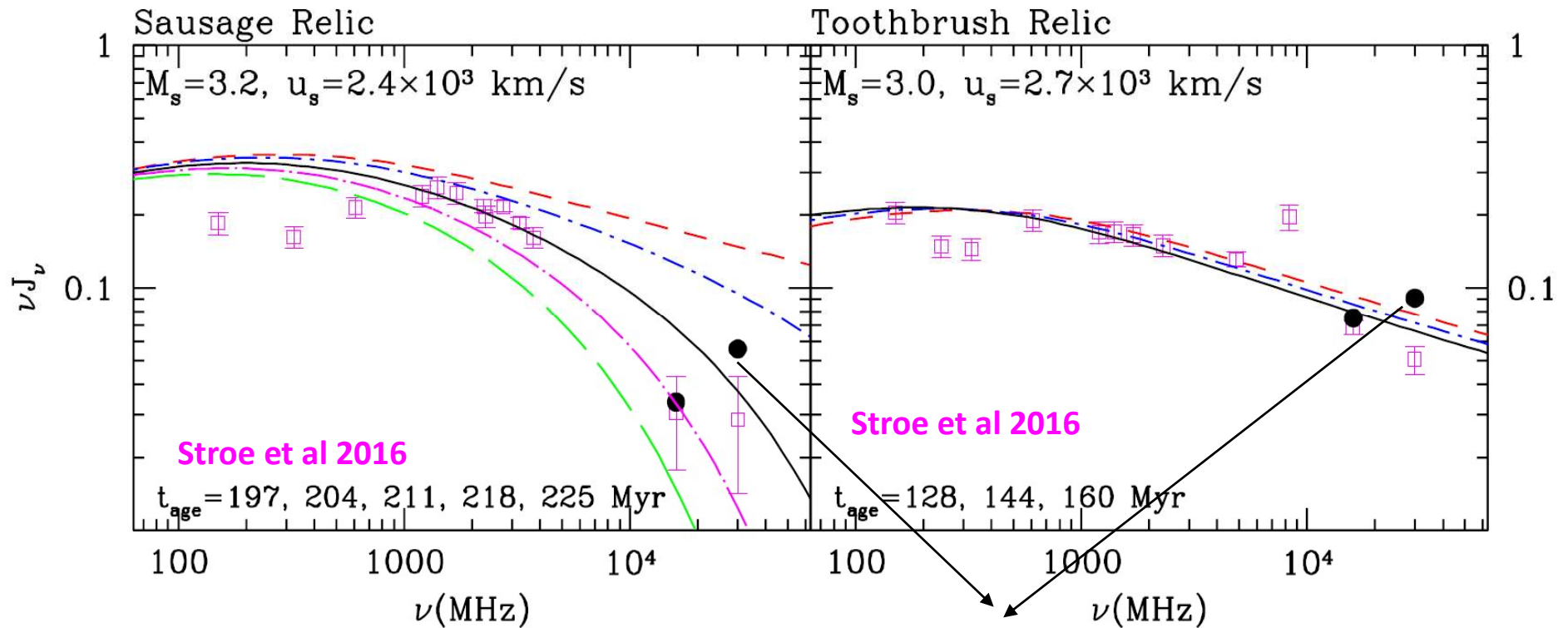


# Fitting of Radio Flux Profiles



**Radiative cooling only**      **Turbulent acceleration with  $\tau_{acc} = 10^8$  yr**

# Fitting of Radio Integrated Spectra



SZ corrected flux by Basu et al. 2016

black solid lines: at time of observations,  $t_{\text{obs}}$

show reasonable agreement with observed data.



## Summary

- Shock Acceleration model with  $M \sim 3$  shock & postshock turbulence acceleration can reproduce observed profiles of radio flux  $S_\nu(R)$  & integrated spectrum  $J_\nu$  of the Sausage and the Toothbrush relic.
- need to understand better the properties of possible turbulence generated behind weak ICM shocks.
- need to study further collisionless shocks in  $\beta=100$  plasma.
- These radio relics provide observational signatures of shocks in galaxy clusters.